Journal of Theoretical and Applied Information Technology
30th November 2014. Vol. 69 No.3

ISSN: 1992-8645 www.jatit.org E-ISSN: 1817-3195

ROBUST ANALYSIS OF THE ROCK TEXTURE IMAGE BASED ON THE BOOSTING CLASSIFIER WITH GABOR WAVELET FEATURES

[1]C.VIVEK, [2]S.AUDITHAN

[1,2]PRIST University, Tanjore, Tamilnadu, India
E-mail: [1]Vivekc.phd@gmail.com , [2]saudithan@gmail.com

ABSTRACT

In this paper, the new novelty method in the digital image analysis technique for geology applications is proposed. It analyzed the series of raw rock images from the mineralogy database of various classes. It initially enhanced for the intensity equalization through HSI model and then the Gabor filter extract the textures of different sizes and orientation in a two dimensional form such as horizontal and vertical directions. The extract features are decomposed through SVD matrix model to achieve better extraction features. The decomposed image features are transformed through the wavelet series and finally, it features are measured using strong boosting classifiers. The experimental results yields better result that compared with other image transformation methods. This proposed method show better classification results for various rock texture images and it cross validated through the confusion matrix and it shows low computational complexity with low error of misclassification.

Keywords: *Rock Texture, HSI, Gabor Wavelet Features, Boosting Classifier and Texton Co-occurrence Matrix*

1. INTRODUCTION

In human vision, the texture classification through imaging applied in many real world scenarios to analyses the type of objects. It applied in various fields including rock classification remote sensing, face detection, tissue classification, the brain tumor classification, printing industries, fabric classification and various biomedical applications that based on the type of texture. Generally, the process of extracting the feature for texture analysis involves statistical, structural and multi-scale methods. The statistical approach for feature extraction gains popularity by the usage of histograms, local binary partition and various co-occurrence matrix pattern and it features are derived from the energy and entropy measures. Then, the features are classified by using various sophisticated machine learning algorithms such as artificial neural network, decision trees, Nearest Neighbor and Boosting algorithms. It process a vast amount of information that selected and transformed via the earlier process and then classify the data based on the heuristic discrimination.

2. LITERATURE SURVEY

Rock image classification is the interesting research in many decades for geological application because the rock possesses multiple properties such as inhomogeneous rock texture, difference in color and granularity properties. The carbonate rocks consists of depositing texture that able to isolate into mudstone, grainstone, wackestone, boundstone and packstone. The process of extracting the texture present in the solid rock image is suggested by Dunham (1962) in [3]. The speckle noise due to higher illumination in rock type images are eliminated with the median value filtering that prevent resolution degradation by Blom & Daily (1982) in [1]. Similarly, the natural surfaces of the images are classified based on the texture through the 3-D fractal surface model and it shows a precise explanation between various surface images by Pentland (1984) in [17]. Later, the texture detection and automatic identification of rock images are analyzed through the co-occurrence matrix method and it show more accurate recognition rate for various size and shape of unique types of rock by Wang (1995) in [20]. The navigation based sonar images to classifying the regions such as sand and rocks based on the fuzzy classifier that refined with

Journal of Theoretical and Applied Information Technology
30th November 2014. Vol. 69 No.3

ISSN: 1992-8645 www.jatit.org E-ISSN: 1817-3195

markov random field model shows significant results by Mignotte et al (2000) in [15]. The advance machine learning algorithms helps to retrieval the rock texture based on the certain classifying features that measured through second order statistics such as co-occurrence matrix. It based on shape, color and texture features to retrieve the images along with the texture directionality features that measured through Hough transform. The Euclidean distance compares the testing image based on feature vectors with higher recall ability. It shows texture resolution plays an important role during analyze the images and achieves an effective classification results that significantly much better than various existing approaches by Lepisto et al (2002) in [10]. In the same way, another rock image low cost implementation system for visual texture inspection woks based on the gray level co-occurrence matrix (GLCM) with selected statistical features for extraction. This method is mainly suitable for homogeneous rock texture classification that implemented by Partio et al (2002) in [16]. It is noted that most of rock deterministic and stochastic texture features are non- homogenous and for classifying it, the spectral features should be primarily focused based on pattern recognition. In the rock image classification method by Lepistö (2003) in [11], the color channels are analyzed through the HSI-model and the features are classified by using the k-nearest neighbor classifier. This method also achieves better result for sub-divided non-homogenous texture image for block classification with reduced misclassification levels. The Gabor filtering plays a major role in HSI color space. The local orientation and scaling is the major distinguish features in texture and the Gabor filtering extract at optimum level that applied in color bands by Lepisto et al (2003) in [9]. Feature extraction method consists of gray level co-occurrence matrix and GMRF features. The classification is done by using Support Vector Machine (SVM). A detailed literature review is presented by Tou et al for the classification of texture images based on various feature extraction techniques. In our previous work [15], we integrated the characterization of textures based on Discrete Shearlet Transform (DST) by extracting entropy measure and to classify the given Brodatz database texture image using K-Nearest Neighbor (KNN) classifier [19]. Although such adaptation improves the classification accuracy, it also severely increases the feature space complexity. Similarly, the an exclusive machine learning algorithm with strong supervised LPBoost classifier to train the ADNI database of MR images in a hyperplane shows improved in classification compared with other methods [8]. Similarly, the LPBoost algorithm optimized for weak classifier while ignoring strong classifier through minimax theory that revokes on the edge constraint shows higher convergence rate and accuracy for real world applications. Later, the same algorithm updated with strong classifier with the limited range that the training set of 5-fold-cross validation shows higher accuracy. [4-5]. It shows from the result that the Gabor filter are most suitable for enhancing as well as reducing the noise while preventing the data loss for the rock texture images and it classified through the LPboosting classifier in this proposed method.

Figure 1. Rock Texture Image of Various Class

3. METHODOLOGY

3.1 HSI Model and Gabor Filter

The HSI color model consists of three components are Hue (H), Saturation (S) and Intensity (I) Hue is the color; Saturation is the intensity of the color and Value or Brightness or Luminosity is the brightness of the color image. Generally, the conversion between the RGB model and the HSI model is quite difficult and it changes the background appearance of the images. The quantities R, G and B are the amounts of the red, green and blue components, normalized to the range [0, 1]. The intensity is just the middling of the red, green and blue components and the angle □ was measured for various rock texture images. The fuzzy clustering of texture based images also plays an important role for extracting the microstructure medical image information that based on the analysis by Vijayakumar et al (2013) in [18]. In the below Figure 2, the process of HSI for rock texture images are performed, initially the raw input image are analyzed for the radiometric and geometric corrections, Then, it applied for HIS image for equalization to achieve better clarity in the pixel regions. The Hue, Saturation and Intensity isolated region of the image are shown below.

Journal of Theoretical and Applied Information Technology
30th November 2014. Vol. 69 No.3

ISSN: 1992-8645 www.jatit.org E-ISSN: 1817-3195

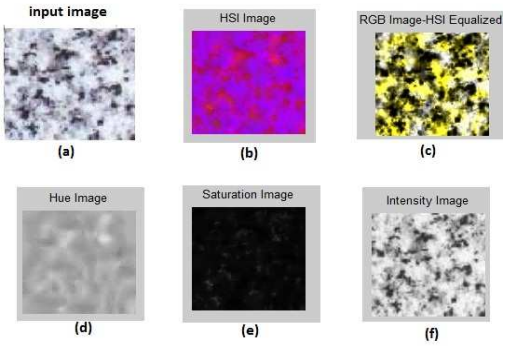

Figure 2. HSI Processing for Rock Texture Images: (a) Input Image, (b) HSI Image, (c) RGB Image - HSI Equalized, (d) Hue Image, (e) Saturation Image and (f) Intensity Image

The RGB based HSI equalized image are used for the filtering in the next stage by using gabor filter. Gabor filters to extract textures of different sizes and orientations (i.e. Gabor-based texture feature). The Gabor filters can be obtained by dilations and rotations of G(x, y).

Assuming that the local regions are spatially homogeneous, we can use the mean, umn, and standard deviation of these regions, σmn, as textural features.

$$\mu_{mn} = \iint \mid W_{mn}(xy) \mid dxdy \quad (1)$$

$$\sigma_{mn} = \sqrt{\iint \mid W_{mn}(xy) \mid -\mu_{mn})^2 dxdy} \quad (2)$$

The general form of 2D Gabor wavelet with an identical modulation frequency of ω at both x and y directions and shift of mx and m y at x and y directions respectively can be as the product of Gabor wavelet in x and y directions in [14].

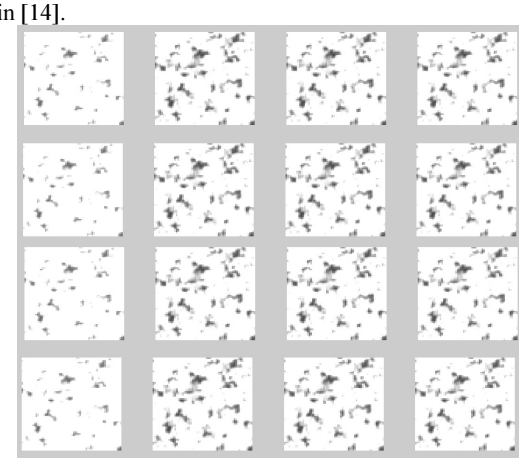

Figure 3. Gabor Filtering of Rock Image Texture On Various Scale Factors

3.2 Singular Value Decomposition

The singular value decomposition, or SVD, is a very powerful and useful matrix decomposition, particularly in the context of data analysis, dimension reducing transformations of images, satellite data etc, and is the method of choice for solving most linear least–squares problems. SVD methods are based on the following theorem of linear algebra (whose proof may be sought elsewhere. The Singular Value Decomposition (SVD). Let A be a real matrix. There exist orthogonal matrices S and C such that

$$\mathbf{A} = \mathbf{S}\boldsymbol{\Sigma}\mathbf{C}^T \quad (3)$$

where S is $m \times m$, C is $n \times n$, and $\boldsymbol{\Sigma}$ is $m \times n$ and has the special diagonal form

when $m > n$ $\boldsymbol{\Sigma} = \begin{pmatrix} \sigma_1 & & 0 \\ & \ddots & \\ 0 & & \sigma_n \\ 0 & \cdots & 0 \\ \vdots & & \vdots \\ 0 & \cdots & 0 \end{pmatrix}$

or when $m < n$ $\boldsymbol{\Sigma} = \begin{pmatrix} \sigma_1 & & 0 & 0 & \cdots & 0 \\ & \ddots & & \vdots & & \vdots \\ 0 & & \sigma_m & 0 & \cdots & 0 \end{pmatrix}$

The entries of $\boldsymbol{\Sigma}$ are ordered in descending order according to

$\sigma_1 \geq \sigma_2 \geq \cdots \geq \sigma_l \geq 0$, where $l = \min\{m, n\}$

The columns of S are called the left–singular vectors, the columns of C the right–singular vectors, and the diagonal elements of $\boldsymbol{\Sigma}$ the singular values of the matrix A. To establish the decomposition given by Equation, we first (matrix) multiply from the right by C to obtain

$$\mathbf{AC} = \mathbf{S}\boldsymbol{\Sigma} \quad (4)$$

The ith column of this relationship is

$$\mathbf{Ac}_i = \sigma_i \mathbf{s}_i \quad (5)$$

for $i = 1, \ldots, n$. It shows that $\mathbf{s}_i$ may be calculated directly from knowledge of $\mathbf{A}$, $\mathbf{c}_i$, and σ_i and the another relation by taking the transpose of equation is

$$\mathbf{A}^T = \mathbf{C}\boldsymbol{\Sigma}^T\mathbf{S}^T \quad (6)$$

Journal of Theoretical and Applied Information Technology
30th November 2014. Vol. 69 No.3

ISSN: 1992-8645 www.jatit.org E-ISSN: 1817-3195

and then (matrix) multiply from the right by S to obtain

$$\mathbf{A}^T\mathbf{S} = \mathbf{C}\boldsymbol{\Sigma}^T \tag{7}$$

The ith column of this relationship is

$$\mathbf{A}^T\mathbf{s}_i = \sigma_i\mathbf{c}_i \tag{8}$$

where again $i = 1,\ldots,n$. Note the above equation shows that $\mathbf{c}_i$ may be calculated directly from knowledge of $\mathbf{A}$, $\mathbf{s}_i$, and σ_i. The associated eigenvalue problems. There are two eigenvalue problems that can be obtained from the SVD. For the first eigenvalue problem we start with equation and multiply from the left by $\mathbf{A}^T$

$$\begin{aligned}\mathbf{A}^T\mathbf{AC} &= \mathbf{A}^T\mathbf{S}\boldsymbol{\Sigma}\\ &= (\mathbf{S}\boldsymbol{\Sigma}\mathbf{C}^T)^T\mathbf{S}\boldsymbol{\Sigma}\\ &= \mathbf{C}\boldsymbol{\Sigma}^T\mathbf{S}^T\mathbf{S}\boldsymbol{\Sigma}\\ &= \mathbf{C}\boldsymbol{\Sigma}^T\boldsymbol{\Sigma}\\ &= \mathbf{C}\boldsymbol{\Sigma}^2\end{aligned} \tag{9}$$

where (assuming $m > n$)

$$\boldsymbol{\Sigma}^2 = \begin{pmatrix}\sigma_1^2 & & 0\\ & \ddots & \\ 0 & & \sigma_n^2\end{pmatrix} \tag{10}$$

Let $\mathbf{R}_1 = \mathbf{A}^T\mathbf{A}$ and $\boldsymbol{\Lambda}_1 = \boldsymbol{\Sigma}^2$, as the eigenvalue problem.

$$\mathbf{R}_1\mathbf{C} = \mathbf{C}\Lambda_1 \tag{11}$$

For the second eigenvalue problem we start with the values and multiply from the left by $\mathbf{A}$

$$\begin{aligned}\mathbf{AA}^T\mathbf{S} &= (\mathbf{S}\boldsymbol{\Sigma}\mathbf{C}^T)\mathbf{C}\boldsymbol{\Sigma}^T\\ &= \mathbf{S}\boldsymbol{\Sigma}\boldsymbol{\Sigma}^T\end{aligned} \tag{12}$$

Let $\mathbf{R}_2 = \mathbf{AA}^T$ and $\boldsymbol{\Lambda}_2 = \boldsymbol{\Sigma}\boldsymbol{\Sigma}^T$, then we can write with the value as the eigenvalue problem

$$\mathbf{R}_2\mathbf{S} = \mathbf{S}\Lambda_2 \tag{13}$$

The Thin SVD is given below,

$$\boldsymbol{\Lambda}_2 = \boldsymbol{\Sigma}\boldsymbol{\Sigma}^T = \begin{pmatrix}\sigma_1 & & 0\\ & \ddots & \\ 0 & & \sigma_n\\ 0 & \cdots & 0\\ \vdots & & \vdots\\ 0 & \cdots & 0\end{pmatrix}\begin{pmatrix}\sigma_1 & & 0 & 0 & \cdots & 0\\ & \ddots & & \vdots & & \vdots\\ 0 & & \sigma_n & 0 & \cdots & 0\end{pmatrix}$$

which generates a square $m \times m$ matrix with diagonal elements

$$\boldsymbol{\Lambda}_2 = \begin{pmatrix}\sigma_1^2 & & 0 & 0 & \cdots & 0\\ & \ddots & & \vdots & & \vdots\\ 0 & & \sigma_n^2 & \vdots & & \vdots\\ 0 & \cdots & \cdots & 0 & \cdots & 0\\ \vdots & & & & \ddots & \vdots\\ 0 & \cdots & \cdots & & \cdots & 0\end{pmatrix}$$

Because the diagonal elements are exploited to analyse the values through the $\Lambda_{kk} = 0 \quad \text{for } k = n+1, \ldots, m$, the eigenvectors (singular vectors) $\mathbf{s}_{n+1}, \ldots, \mathbf{s}_m$ are of no importance. As a result we define a new $m \times n$ matrix $\hat{\mathbf{S}}$ (it is $\mathbf{S}$ with the last $m-n$ columns deleted) and a new $n \times n$ diagonal matrix $\hat{\boldsymbol{\Sigma}}$ (whose diagonal elements are $\sigma_1, \ldots, \sigma_n$) and write the thin SVD (or reduced SVD) of A that proposed in [6].

$$\mathbf{A} = \hat{\mathbf{S}}\hat{\boldsymbol{\Sigma}}\mathbf{C}^T \tag{14}$$

3.3 Texton Co-Occurrence Matrix

The overall combination of the proposed system diagram is given in Fig 3.4. In a gray level image, the texton co-occurrence matrix (TCM) differentiates the features of pixel based on the interrelation to the textons. Let g be the unit vector corresponding to the G of the gray level in the image, then the following vectors co-ordinate with the function f(x, y) [12, 13]:

$$u = \frac{\partial G}{\partial x}g \tag{15}$$

$$v = \frac{\partial G}{\partial y}g \tag{16}$$

The dot products to the above vectors are given below:

$$g_{xx} = u^{\mathbf{T}}u = \left|\frac{\partial G}{\partial x}\right|^2 \tag{17}$$

$$g_{yy} = v^{\mathbf{T}}v = \left|\frac{\partial G}{\partial y}\right|^2 \tag{18}$$

$$g_{xy} = u^{\mathbf{T}}v = \frac{\partial G}{\partial x} \bullet \frac{\partial G}{\partial y} \tag{19}$$

The $\theta(x, y)$ is the direction that changes with the vectors:

Journal of Theoretical and Applied Information Technology
30th November 2014. Vol. 69 No.3

ISSN: 1992-8645 www.jatit.org E-ISSN: 1817-3195

$$\theta(x,y)=\frac{1}{2}\tan^{-1}[\frac{2g_{xy}}{(g_{xx}-g_{yy})}] \quad (20)$$

To identify the value ranges $C(x,y)$ from lower value to higher value of 0 to 255, the $G(x,y)$ is given below:

$$G(x,y)=\{\frac{1}{2}[(g_{xx}+g_{yy})+(g_{xx}-g_{yy})\cos 2\theta+2(g_{xy}\sin 2\theta)]\}^{\frac{1}{2}} \quad (21)$$

The texton templates [12, 13] consists of five types of unique frames to identify the textons that illustrated in Fig.3.4.

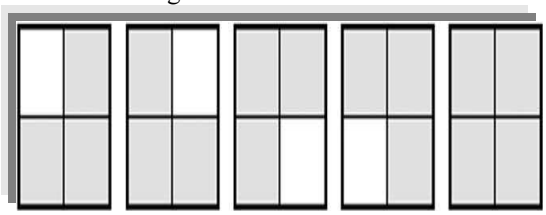

Figure 4. Texton Templates with Five Unique Types

To identify the texton in the original image, the texton templates are morphed the input image on various texton location that generate the five unique combination of texton component images. Finally, the component images are combined together into texton identified image by enumerating the boundary for all morphed regions that shown in Fig 3.4 The texton image T with the adjacent pixels as well as and its corresponding weight of the pixels. Similarly, the orientation angle of the image indicated. Then, the group of texton image are undergoes to shearlet transform that decompose the image.

3.4 Discrete Wavelet Transform

The image expanded in a multiple layer that considered as models of a continuous function. That engraves as the discrete wavelet transform (DWT) that based on

$$f(x)=\sum_k c_{j_0}(k)\phi_{j_0,k}(x)+\sum_{j=j_0}^{\infty}\sum_k d_j(k)\psi_{j,k}(x) \quad (22)$$

where j_0 is an arbitrary starting scale and the $c_{j_0}(k)$'s are normally called the approximation or scaling coefficients. The fast wavelet transform (FWT) is a computationally efficient implementation of the discrete wavelet transform (DWT) that exploits the relationship between the coefficients of the DWT at adjacent scales in [13].

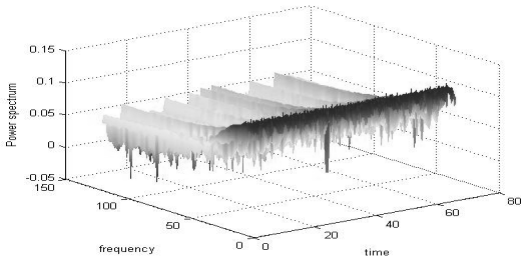

Figure 5. Wavelet Transformation Visualization Factor

4. PROPOSED WORK

The boosng classifier optimizes the classification based on edges. The LPboost strong classifier focus on the weak classifier for the extracted features based on the shearlet transform relative entropy. It bounds as the edges of the strong classifier in which are lesser for minimum edges based on the convergence rate. The distributions of the edge margin are linear for training the set of images based on the similar features. The entropy regularized parameters for the feature vector, to update the distribution clearly. Based on the mini-max theory that eliminates the error in classifying though error matrix that shown in Figure 6.

	h_1	...	h_n	$\overline{d}$
x_1	$u_{1,1}$	...	$u_{1,n}$	d_1
...	...	...	...	...
x_m	$u_{m,1}$	...	$u_{1,n}$	d_n
$\overline{w}$	W_1	...	W_n	

Figure 6. Error Matrix in the Training Sets

In the Error matrix, the training sets X={ x1, x2, x3…xm } and is the distribution of various training sets from d1, d2, d3…dn with the distribution of the hypothesis from w1, w2, w3…wn that based on the features that manipulated with the hypothesis for each sample sets h1, h2, h3…hn. The minimax theory suggests the edge constraints based on its relative entropy through the feature extracted region. It helps to solve the weak classifier optimization effectively.

Journal of Theoretical and Applied Information Technology
30th November 2014. Vol. 69 No.3

ISSN: 1992-8645 www.jatit.org E-ISSN: 1817-3195

$$f^{t}(x) = \sum_{q=1}^{t} w_q h^{q}(x).$$

$$\min_{d_t, \gamma} \gamma + \eta . \Delta \left(\overline{d}_t, \overline{d}_0 \right)$$

$$s.t \sum_{i=1}^{m} u_{i,j} d_i \le \gamma, \quad \text{for } 1 \le j \le t;$$

$$\sum_{i=1}^{m} H'_{t-1}(x_i)\, y_i\, d_i \le \gamma;$$

$$0 \le d_j \le \frac{v}{m}, \sum_j d_j = 1; \qquad (23)$$

The main advantages of using LPboost classifiers are it performs train sequentially for the weak classifiers based on the preceding rules. It reduces the complication based on its hypotheses. The discriminate functions based on the LPboosting classification reduce the redundancy and misclassification. Based on the error matrix, the misclassification reduced with constant iteration that shown in the Fig 4.2. The classification rates abruptly increases as the training sets feature increases. It predominantly shows the efficient classification in the training images. Similarly, the collection of test images which identified by the subset homogenous pattern for classification. It improves the calculation and classification performance which shown in the below Figure 7.

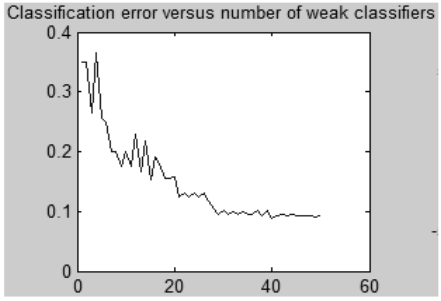

Figure 7.The Misclassification to the Weak Classifier in LPboosting Classifier

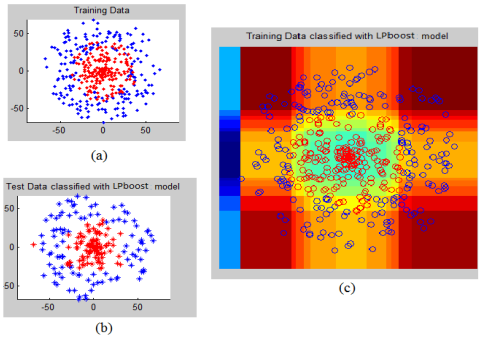

Figure 8. LPboosting Classification on the Texture Images: (a) Training Data, (b) Test Data Classified with LPboost Model, (c) Training Data Classified with LPboost Model

5. EXPERIMENTAL RESULT AND DISCUSSION

In this analysis, the rock texture image of various set are taken and it divided into class 1 to class 10. It consist of total images of 50 rock texture images. The Mineralogy database acts as quantitative lithology interpretation [7] consists of multiple type of mineral species and in this analysis, the raw images with higher tolerance and major composition of crystal images are analyzed. The rock image classification accuracy of the proposed system is evaluated using the evaluation metrics, such as sensitivity, specificity and accuracy that based Zhu et al. (2010) is defined. Based on the confusion matrix, the error in the LPboosting classifier are clearly shown for various Rock texture image classes. It is noted that the performance of the algorithm efficiently improved when the machine classifier analyze the Rock texture images in the "class 5". The similarity of " class 5" to compare with other classes image are significantly reduced during the process of retrieving the "class 5" images. The performance evaluations of the proposed texture classification system are identified. From each original image, 128x128 pixel sized images are extracted with an overlap of 32 pixels between vertical and horizontal direction. From a single 640x640 texture image, 256 128x128 images are obtained

$$Sensitivity = TP/(TP + FN)$$

$$Specificity = TN/(TN + FP)$$

$$Accuracy = (TN + TP)/(TN + TP + FN + FP) \qquad (24)$$

Where stands for True Positive, stands for True Negative, stands for False Negative and stands for False Positive. As suggested by above equations. Based on the measurements through the

Journal of Theoretical and Applied Information Technology
30th November 2014. Vol. 69 No.3

ISSN: 1992-8645 www.jatit.org E-ISSN: 1817-3195

statistical parameters such as sensitivity, specificity and accuracy for the analysis of texture features based on the classifier. The sensitivity deals with the probability of true postive prediction whereas the specificity is the probability of true negative prediction to conclude the original condition of the images.

Table 1 Comparison of the Various Evaluation Metrics with the Proposed System

Evaluation metrics		LPboosting+DCT	LPboosting+DST	LPboosting+DWT
Input rock texture images for various classes	TP	37	35	38
	TN	8	8	9
	FP	2	2	1
	FN	3	5	2
	Sensitivity	0.925	0.875	0.95
	Specificity	0.73	0.62	0.9
	Accuracy	0.9	0.86	0.94
	Total error(%)	10	14	6

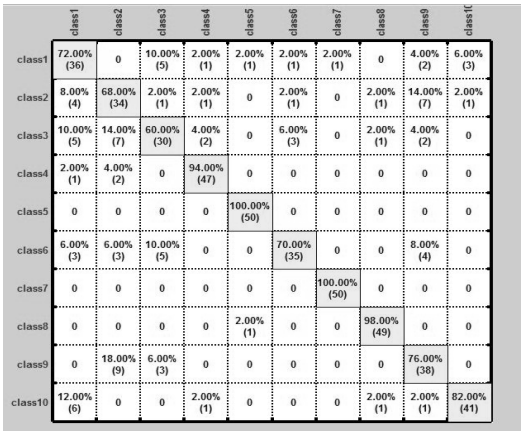

Figure 9. Confusion Matrix Analysis for the Proposed Rice Texture Analysis Method

But, accuracy is the level of exactness based on the given set of images. In the above Table 5.1, the sensitivity of the proposed LPboosting+DWT approach is better compared to other methods LPboosting+DST and LPboosting+DCT. The specificity for the proposed design LPboosting+DWT leads by 0.17% and 0.28% of the existing LPboosting+DST and LPboosting+DCT method respectively. Similarly, the accuracy of LPboosting+DWT is extremely higher than all other approaches. Based on the experimental results, the proposed system classification error rate is less than the other classifier; it is shown in Figure 3.15. It is seen that the proposed method error ratio is only 7.5% for rock image datasets whereas the LPboosting+DCT and LPboosting+DST methods have error rate of 12.5% and 17.5% respectively. Compared to existing methods, the proposed LPboosting+DWT algorithm is much sophisticated for the classification of rock texture images.

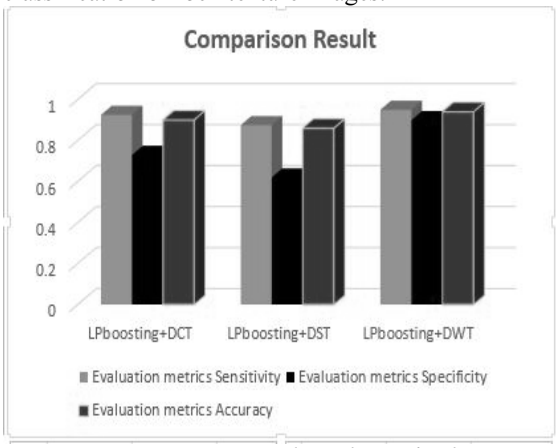

Figure 10. Comparison Result Analyses of LPboosting with DCT, DST and DWT

The texture description for the natural rock images has been extracted using gabor filtering to inspect the surface of rock plates. It helps to detect the orientation and strength of crack regions in the surface of the rock image. Since, it is color based extraction, the beneficial of extraction information in high dimensional descriptors. It helps to seperate the individual base classification more clearly.

Journal of Theoretical and Applied Information Technology
30th November 2014. Vol. 69 No.3

ISSN: 1992-8645 www.jatit.org E-ISSN: 1817-3195

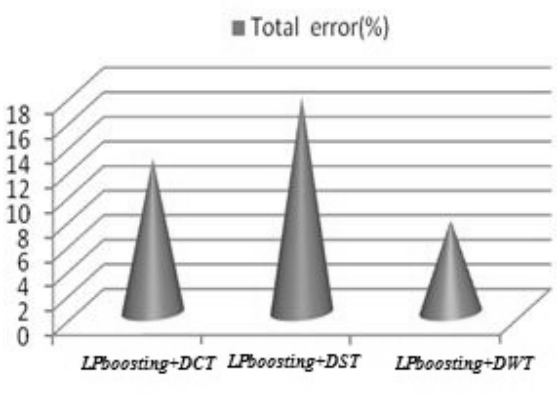

Figure 11. Comparison Error Bar of the Existing and Proposed LPboosting Classifier with Various Transform Methods.

6. CONCLUSION AND FUTURE ENHANCEMENTS

In this paper, the trend of classifying the rock images from mineralogy database as the highlighted applications. It successfully enhanced through HSI model and then feature are extracted Gabor wavelet features while decomposing the images. The decomposition of image are manipulated through the texton co-occurrence matrix and it processed with the discrete wavelet transformation. It shows maximum level of feature extracted that classified using the advance strong LPboosting classifier. The classifier yields better result of accuracy of 0.94 % that compared with other advance image transformation methods. It shows the proposed method leads by 0.17% and 0.28% of other existing method such as DST and DCT. It significantly achieve better results with low misclassification level that cross validation using confusion matrix. In the future we will investigate other statistical texton based operators, such as local patch to further improve recognition accuracy by their fusion. The texture description for the natural rock images has been extracted using gabor filtering to inspect the surface of rock plates. It helps to detect the orientation and strength of crack regions in the surface of the rock image. Since, it is color based extraction, the beneficial of extraction information in high dimensional descriptors. It helps to seperate the individual base classification more clearly. In future, the proposed algorithm will be utilized for the medical related microtexture imaging applications such as stain images and lab images. This concept can be utilized in text extraction because the advance wavelet transform combined to extract the features in the image very significantly. Moreover, this application requires less time to process and it will have many importance to medical imaging applications such as CT, MRI scanning for brain tumor, breast cancer, retinopathy segmentation and classification.

REFRENCES:

[1] Blom, R & Daily ., "Radar image processing for rock-type discrimination", IEEE Transactions onGeoscience and Remote Sensing, vol. 3,pp. 343-351, 1982.

[2] Carper, W., "The use of intensity-hue-saturation transformations for merging SPOT panchromatic and multispectral image data", Photogrammetric Engineering and remote sensing, vol. 56, no. 4, pp. 459-467, 1990.

[3] Dunham, R., "Classification of carbonate rocks according to depositional textures", AAPG Special Volumes, pp. 108-121, 1962

[4] Fang, Y, Fu, Y, Sun, C, & Zhou, J., "Improved Boosting Algorithm Using Combined Weak Classifiers", Journal of Computational Information Systems, vol. 7, no. 5, pp. 1455-1462,=2011.

[5] Fang, Y. K, Fu, Y, Sun, C. J, & Zhou, J.,"LPBoost with Strong Classifiers", International Journal of Computational Intelligence Systems, vol. 3 no. 01, pp. 88-100, 2010.

[6] Golub, G, & Reinsch, C., "Singular value decomposition and least squares solutions", Numerische Mathematik, vol. 14, no. 5, pp. 403-420. 1970.

[7] Herron, M, & Herron, S "Quantitative lithology: open and cased hole application derived from integrated core chemistry and mineralogy database", Geological Society, London, Special Publications, vol. 136, no. 1, pp. 81-95, 1998.

[8] Hinrichs, C, Singh, V., Mukherjee, L., Xu, G, Chung, M. K, & Johnson, S., "Spatially augmented LPboosting for AD classification with evaluations on the ADNI dataset", Neuroimage, vol. 48, no. 1, pp. 138-149, 2009.

[9] Lepisto, L., Kunttu, I., Autio, J, & Visa, A., "Classification method for colored natural textures using gabor filtering", Proceedings. IEEE 12th International Conference In Image Analysis and Processing, Chicago, pp. 397-401, 2003.

ISSN: 1992-8645 www.jatit.org E-ISSN: 1817-3195

[10] Lepisto, L., Kunttu, I, Autio, J & Visa, A., "Comparison of Some Content-Based Image Retrieval Systems with Rock Texture Images", In Proceedings of 10th Finnish Artificial Intelligence Conference, Oulu, Finland, pp. 156-163, 2002.

[11] Lepistö, L., Kunttu, I, Autio, J, & Visa, A., "Rock image classification using non-homogenous textures and spectral imaging", 2003.

[12] Liu, G, Zhang, L., Hou, Y, Li, Z. Y, & Yang, J., "Image retrieval based on multi-texton histogram", Pattern Recognition, vol. 43, no. 7, pp. 2380-2389, 2010.

[13] Liu, G. H., Li, Z. Y., Zhang, L., & Xu, Y. (2011). "Image retrieval based on micro-structure descriptor". Pattern Recognition, 44(9), 2123-2133.

[14] Ma, L., Wang, Y, & Tan, T., " Iris recognition based on multichannel Gabor filtering", In Proc. Fifth Asian Conf. Computer Vision, Vol. 1, pp. 279-283, 2002.

[15] Mignotte, M., Collet, C, Pérez, P., & Bouthemy, P., "Markov random field and fuzzy logic modeling in sonar imagery: application to the classification of underwater floor", Computer Vision and Image Understanding, vol. 79, no. 1, pp. 4-24, 2000.

[16] Partio, M, Cramariuc, B, Gabbouj, M, & Visa, A., "Rock texture retrieval using gray level co-occurrence matrix", In Proc. of 5th Nordic Signal Processing Symposium, Vol. 75, 2002.

[17] Pentland, A., "Fractal-based description of natural scenes", Pattern Analysis and Machine Intelligence, IEEE Transactions on, vol. 6, pp. 661-674, 1984.

[18] Vijayakumar, B, Chaturvedi, A, & Kumar, KM., "Effective Classification of Anaplastic Neoplasm in Huddling Stain Image by Fuzzy Clustering Method", International Journal of Scientific Research, vol. 3, 2013.

[19] Vivek, C. & Audithan, S., "A novelty approach of spatial co-occurrence and discrete shearlet transform based texture classification using LPboosting classifier", Journal of computer science, vol. 10, pp. 783-793, 2014.

[20] Wang, L.., "Automatic identification of rocks in thin sections using texture analysis", Mathematical geology, vol. 27, no. 7, pp. 847-865, 1995.

[21] Wong, S., Zaremba, L., Gooden, D, & Huang, H., "Radiologic image compression-a review", Proceedings of the IEEE, vol. 83, no. 2), pp. 194-219. 1995.

[22] Zhu, W, Zeng, N, & Wang, N. "Sensitivity, specificity, accuracy, associated confidence interval and ROC analysis with practical SAS® implementations", NESUG proceedings: health care and life sciences, Baltimore, Maryland. 2010.